

Transfer of patterned ion-cut silicon layers

C. H. Yun, A. B. Wengrow, and N. W. Cheung

Electronics Research Laboratory, University of California Berkeley, Berkeley, California 94720

Y. Zheng, R. J. Welty, Z. F. Guan, K. V. Smith, P. M. Asbeck, E. T. Yu, and S. S. Lau

Department of Electrical and Computer Engineering, University of California San Diego, La Jolla, California 92093

(Received 5 August 1998; accepted for publication 28 August 1998)

The technique of transferring patterned ion-cut layers from one Si wafer to another was demonstrated. The starting silicon wafer was masked with checkerboard and line patterns with a $3\ \mu\text{m}$ thick polymethylmethacrylate/photoresist and was implanted with $5 \times 10^{16}\ \text{H}^+$ ions/ cm^2 at 150 keV. After stripping off the mask, the wafer was bonded to an oxide-coated receptor wafer through low-temperature direct wafer bonding. Heat treatment of this bonded pair showed that the hydrogen-induced silicon surface layer cleavage (ion cut) could propagate throughout about $16\ \mu\text{m} \times 16\ \mu\text{m}$ of nonimplanted material with implanted regions only $4\ \mu\text{m}$ wide. Mask width, spacing, and implantation profiles through the mask shape were shown to have effects on the internal microfracturing mechanisms. © 1998 American Institute of Physics.

[S0003-6951(98)00645-7]

Three-dimensional electronic device integration offers significant opportunities for future system improvement in microprocessors and memories.^{1,2} This prospect might be implemented with the hydrogen-induced silicon layer cleavage process, which has already been reported for capacitor patterns (passive devices).³ To cleave the implanted layer, a minimum dose of a few times $10^{16}/\text{cm}^2$ of implanted hydrogen is needed.⁴ This large dose of hydrogen most likely will damage the devices fabricated on the silicon prior to the ion-cut process. In this study, we introduce a patterned ion-cut process in which active regions of the wafer are protected from the hydrogen implantation.

In this study, Czochralski-grown, (100), *n*-type ($\rho = 5\text{--}50\ \Omega\ \text{cm}$), 100 mm silicon wafers were used. The Si donor wafer was coated with a layer of KTI 950K 9% polymethylmethacrylate (PMMA) and a layer of Shipley 1400-30 photoresist with a total thickness of $3\ \mu\text{m}$, followed by patterning of various sizes of squares and lines for the implantation mask with different openings for the hydrogen implantation (see Fig. 1). This patterned wafer was then implanted with H^+ ions at 150 keV with a dose of $5 \times 10^{16}\ \text{cm}^{-2}$. Dur-

ing implantation, the wafer was kept at ambient temperature. A $3\ \mu\text{m}$ thick ion mask layer (including PMMA and the photoresist) was applied to prevent the hydrogen ions from reaching the silicon wafer surface, resulting in hydrogen-ion implantation only in the openings. After the implantation, the ion mask was removed by oxygen plasma ashing. To determine the cracking temperature, the patterns were annealed at temperatures from 400 to 600 °C in forming gas for 5 min after the removal of the ion mask. It was found that blistering occurred between 500 and 550 °C. It was clear under the microscope that all the blisters were confined to the implanted regions. This observation confirms the effectiveness of the implant mask for the protected regions.

On the receptor wafer, a layer of thermal oxide 200 nm thick was grown. The two wafers were bonded directly face-to-face at room temperature or at slightly elevated temperature after standard RCA cleaning of the implanted wafer. The bonded pair was then heated in a rapid thermal annealer until cracking took place, typically, between 500 and 550 °C. This process enables the transfer of a silicon layer with an average thickness of $1.3\ \mu\text{m}$ from the donor wafer to the receptor wafer. Figure 2 shows schematically the patterned ion-cut process flow.

Figures 3 and 4 show optical micrographs and atomic

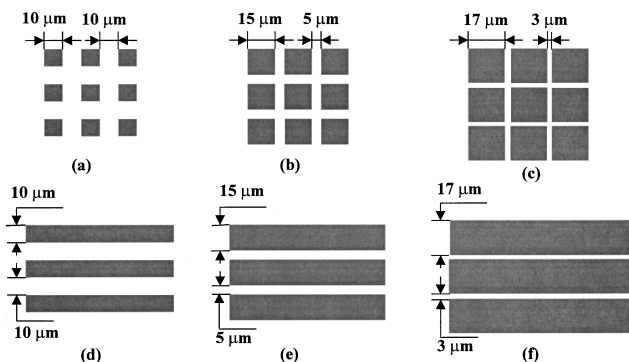


FIG. 1. Implantation mask patterns (a)–(f). The shaded regions are the ion masks. Due to limitations of lithography, the actual size of the ion masks is smaller than those shown. Please refer to Figs. 3, 4, and 5 for details.

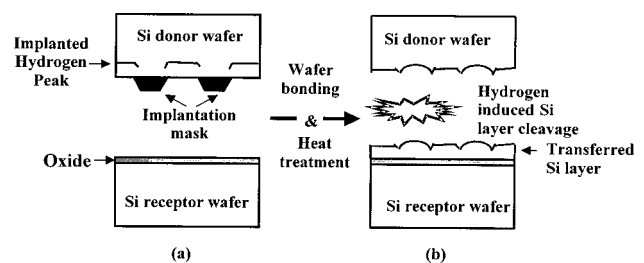


FIG. 2. Process flow for patterned ion cut. Note the effect of the slope of the ion mask near the edge on the hydrogen distribution. The inclined distribution of implanted H near the edge of the ion mask induces the inclined initial ion cut shown in Figs. 4 and 5.

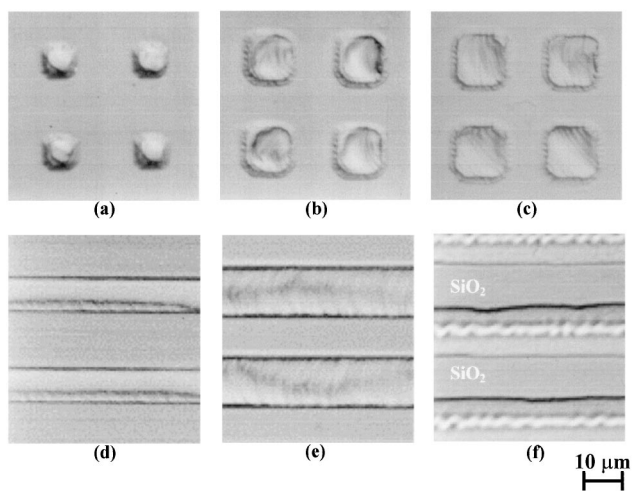


FIG. 3. Optical micrographs of transferred silicon layer surfaces. The non-implanted regions are successfully transferred to the receptor wafer, except pattern (f). In (f), the exfoliation went all the way down to the SiO₂ surface.

force micrographs (AFM) of the surface topography of the transferred layer surfaces, respectively. In Fig. 3, the regions with larger roughness are the nonimplanted areas. It should be pointed out that the rough regions were smaller than the measured photoresist mask boundaries after implantation. For example, in pattern (c) the area of the ion mask was measured to be about 16 μm×16 μm [also see Fig. 4(c)], while the rough area is only 14 μm×14 μm. Each pattern used in the experiment, except (f), was successfully cleaved. As shown in Fig. 4, the topography of most of these patterns

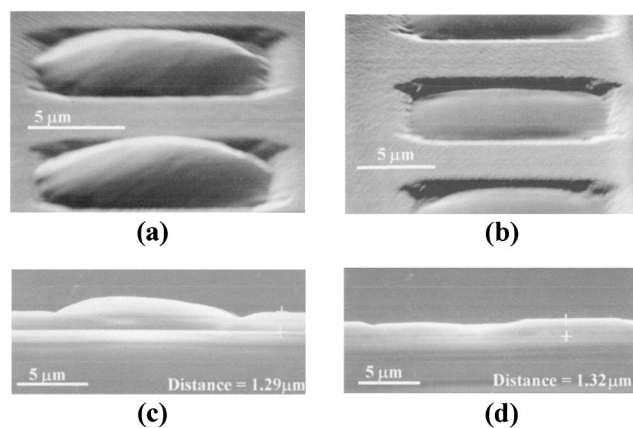


FIG. 5. SEM micrographs of ion mask pattern (b) after exfoliation. (a) and (b) are taken at a tilt angle of about 70°. (c) and (d) are cross-sectional images, corresponding to (a) and (b), respectively. These two kinds of exfoliation are the dominant features for pattern (b).

shared a common feature in that the AFM scan shows a similar exfoliation curve, except for patterns (a) and (f). This phenomenon was further studied using scanning electron microscopy (SEM) on the transferred layer of pattern (b) (see Fig. 5).

There are two dominant features of the nonimplanted areas for pattern (b), as shown in Figs. 5(a) and 5(b); corresponding cross-sectional images are shown in Figs. 5(c) and 5(d), respectively. The cross-sectional view showed that the thickness of the exfoliated layer in the implanted regions was about 1.3 μm, in good agreement with the projected range of

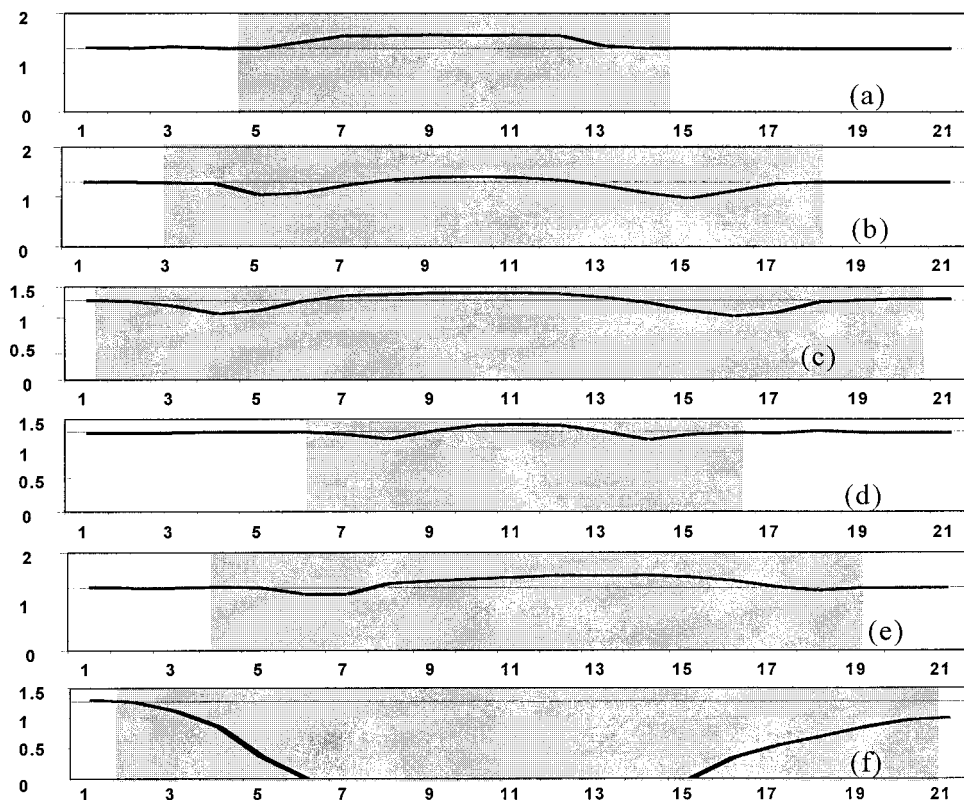


FIG. 4. Silicon layer thickness vs horizontal position around the nonimplanted region using an AFM scan. The nonimplanted areas are shaded, and the average thickness of the silicon overlayer is shown as thin lines. For each sample, the scanned distance was 22 μm across the exfoliated areas. The scanning was done in the high-resolution mode. The horizontal scale was chosen to show the entire scanned distance. All units are in micrometers.

1.3 μm predicted by the TRIM96 code. In the nonimplanted regions, the exfoliation was initiated along the ion mask edge and propagated horizontally for 1–2 μm , and cleaved downward (towards the Si layer surface) to a depth of about 0.2–0.3 μm , followed by three competing tendencies: (i) the exfoliation went upward and the cuts merged near the center of the implanted region [Figs. 4(b)–4(e) and Figs. 5(a)–5(c)]; (ii) the exfoliation went across the (100) plane [Figs. 5(b) and 5(d)]; and (iii) occasionally the exfoliation continued downwardly and went all the way down to the SiO₂ surface [Fig. 4(f)]. In this case, the nonimplanted Si region did not transfer to the receptor wafer. In Fig. 4(a), the downward cleave was not as obvious as the others.

We have explained these internal fracture propagation observations with the following scenarios. First, stress localization from the cleavage front due to blistering of the surrounding implanted region propagates the crack on the cleavage plane inward. The initial downward motion can be attributed to the fact that the ion mask had a finite slope due to resist exposure, development, and implantation erosion. Implantation through a sloped mask brings the band of implanted hydrogen towards the surface, resulting in the initial downward cut (see Fig. 2). The implanted hydrogen tends to form platelets primarily on (100) and occasionally on the (111) planes,⁵ however, the favored cleavage planes of silicon crystal are the (111) planes. These two conflicting factors then determine the exfoliation directions in our case. We believe that near the implanted edge the majority of the (100) platelets tend to trigger exfoliation along the (100) plane,

while the existence of the (111) platelets and the (111) planes, being the cleavage planes, are the driving force for the upward or downward cut. It is unclear why the upward exfoliation is preferred rather than the downward exfoliation at the present time. Further study is needed to fully understand this phenomenon.

In summary, we have demonstrated a technique of transferring patterned ion-cut layers, which can be useful for three-dimensional chip integration or layer transfer techniques. Square and line patterns were successfully transferred to the receptor wafer. As shown in this work, 16 $\mu\text{m} \times 16 \mu\text{m}$ of the masked area can be cleaved by implanting hydrogen in only 4 μm of the opening region around it.

Work performed at UCB was supported by the NSF and the California State MICRO program. The UCSD acknowledges the financial support of the NSF. One of the authors (E.T.Y.) would like to acknowledge financial support from the Alfred P. Sloan Foundation.

¹M. B. Kleiner, S. A. Kühn, P. Ramm, and W. Weber, *IEEE Trans. Compon., Packag. Manuf. Technol., Part B* **19**, 709 (1996).

²S. Nakamura, H. Horie, K. Asano, Y. Nara, T. Fukano, and N. Sasaki, *Tech. Dig. Int. Electron Devices Meet.*, 889 (1995).

³B. H. Lee, G. J. Bae, K. W. Lee, G. Cha, W. D. Kim, S. I. Lee, T. Barge, A. J. Auberton-Herve, and J. M. Lamure, *IEEE SOI Conf.*, 114 (1996).

⁴M. Bruel, *Nucl. Instrum. Methods Phys. Res. B* **108**, 313 (1996).

⁵Q.-Y. Tong, R. Scholz, U. Gösele, T.-H. Lee, L.-J. Huang, Y.-L. Chao, and T. Y. Tan, *Appl. Phys. Lett.* **72**, 49 (1998).